Geosciences and Engineering, Vol. 12, No. 2 (2024), pp. 82–92.
https://doi.org/10.33030/geosciences.2024.02.007

ANALYSES OF GRAPHITE-BEARING SCHISTS FROM FERTŐRÁKOS, SOPRON MTS., NW-HUNGARY

LÍVIA LESKÓNÉ MAJOROS[1]*, MÁTÉ ZS. LESKÓ[2], KRISZTIÁN FINTOR[3], DÉLIA BULÁTKÓ-DEBUS[4], FERENC MÓRICZ[5], SÁNDOR SZAKÁLL[6], FERENC KRISTÁLY[7]

[1, 2, 4, 5, 6, 7]*Institute of Exploration Geosciences, University of Miskolc, Hungary*
[3]*Department of Geology, University of Szeged, Hungary*
[1]*livia.leskone@uni-miskolc.hu
[2]mate.lesko@uni-miskolc.hu
[3]fintor.krisztian@szte.hu
[4]delia.bulatko-debus@uni-miskolc.hu
[5]ferenc.moricz@uni-miskolc.hu
[6]sandor.szakal@uni-miskolc.hu
[7]ferenc.kristaly@uni-miskolc.hu

Abstract: Potential graphite-bearing schists are investigated from Fertőrákos (Sopron Mts., NW-Hungary) with ore microscopy, scanning electron microscopy, Raman spectroscopy, X-ray powder diffraction and X-ray fluorescence spectrometry. Disordered graphite is identified by Raman spectroscopy, which appears as <50 μm sized flakes, and as 50–300 μm sized lens-shaped granular aggregates in the deformed zones of the samples detected by ore and scanning electron microscopy. Using graphite geothermometry on Raman spectra, the average formation temperature of the Fertőrákos samples is ~440 °C (±50 °C).

Keywords: *graphite, Raman spectroscopy, graphite geothermometry, greenschist facies metamorphism, shear zone*

1. INTRODUCTION

Graphite plays an ever-growing role nowadays and is also a critical raw material as included on the List of Critical Raw Materials for the European Union since 2011 (Study on the Critical Raw Materials, 2023). It is worth being aware of potential graphite occurrences in Hungary, and modern analytical techniques (such as Raman spectroscopy) enable detailed examination of graphite and graphitized material.

Recently, graphite occurrences were examined in the NE region of Hungary: Dédestapolcsány from the Uppony Mts. (Majoros, 2019), Meszes (Leskó Majoros et al., 2021) and Szendrőlád (Majoros et al., 2022) from the Szendrő Mts. Generally, the graphite-bearing rocks are siliceous black schists (Dédestapolcsány) or black phyllites (Meszes and Szendrőlád) that have ~1–4 weight% graphite content. Dédestapolcsány samples contain μm sized graphite flakes and 100–300 μm sized grains, Meszes samples have 50–150 μm sized flakes, while Szendrőlád samples contain 20–50 μm sized flakes (Leskóné Majoros et al., 2022).

However, in the NW part of Hungary, graphite exploration was carried out only during the early 1980s. Notably, Kósa and Fazekas (1981) conducted investigations in

the Sopron Mountains. According to their findings, in the Fertőrákos Metamorphic Complex, carbonization-graphitization in the micaschists is a common phenomenon, the degree of carbonization ranges from coal that does not reach the anthracite state to graphite. Based on their observations, the presence of graphite in the assemblage is always related to structurally highly stressed zones and planes; graphite is considered as a tectonite (Kósa and Fazekas, 1981).

Our aim was to collect samples and examine them with several analytical methods (ore microscopy, scanning electron microscopy, Raman spectroscopy, X-ray powder diffraction and X-ray fluorescence spectrometry) to get further detailed information about the graphitized material.

2. MATERIALS AND METHODS

Rock samples were collected from surface outcrops from the southern slope of Újhegy, located 3 km north of the village of Fertőrákos in the Sopron Mountains. The exact coordinates are EOV X_1: 268 936, EOV Y_1: 470 099 (outcrop 1) and EOV X_2: 268 917, EOV Y_2: 470 083 (outcrop 2). The collected graphitic schists belong to the Fertőrákos Metamorphic Complex.

The age of the Complex is early Carboniferous–early Permian, the rocks were affected by greenschist facies metamorphism. Petrologically, it is graphite-bearing phyllite and paragneiss with amphibole schist bodies and frequent pegmatite lenses of high (70–80%) apatite content. Structurally, it is part of the Austroalpine nappe system, overlained by the Sopron Metamorphic Complex with a tectonic boundary (Babinszki et al., 2024). *Figure 1* shows the map of Hungary with Fertőrákos village (Sopron Mts.), the schematic geological map of the investigated area, the surface outcrops and the collected rock samples.

Polished rock slabs were made for ore microscopy (OM), scanning electron microscopy (SEM-EDX) and Raman spectroscopy. The OM examinations were carried out on a Zeiss Axio.Imager A2.m polarizing petrographic and ore microscope with Zeiss AxioCam MRc5 camera. The SEM-EDX measurements were made on a JEOL JXA-8600 Superprobe instrument (in high vacuum at 20 kV, beam current of 20 nA, 60 s dwell time for point analysis). Detection limit of the EDX system for light elements is 0.1 weight%, for heavy elements is 0.05 weight%, the limit of measurement error is 5 relative%. The Raman spectroscopy analyses were carried out on a Thermo Fisher Scientific DXR Raman microscope (532 nm wavelength (green) laser, 2 mW laser power, 3 × 15 s exposure time, ~4 cm^{-1} spectral resolution).

Powder samples were made for X-ray powder diffraction (XRD) and X-ray fluorescence spectrometry (XRF). The XRD measurements were carried out on a Bruker D8 Discover instrument (Cu K-alfa radiation, 40 kV, 40 mA, Bragg-Brentano geometry, LynxEye XE-T PSD detector with 2° opening, 0.007°2θ/24sec counting time). Crystalline phase identification was made in Diffrac*Plus* EVA software by Search/Match algorithm on ICDD PDF2 (2005) database. Rietveld refinement was made with empirical instrument parameterization on NIST SRM640d Si standard in TOPAS4 software, while crystal structure data for calculations were obtained from AMCSD (Downs and Hall-Wallace, 2003) database. The XRF analyses were made

on a Rigaku SuperMini200 WDS instrument (LiF200 / PET / XR25 crystals), with Pd cathode (200 W, 50 kV accelerating voltage, 4 mA beam current) on powder samples pressed into CereOx powder.

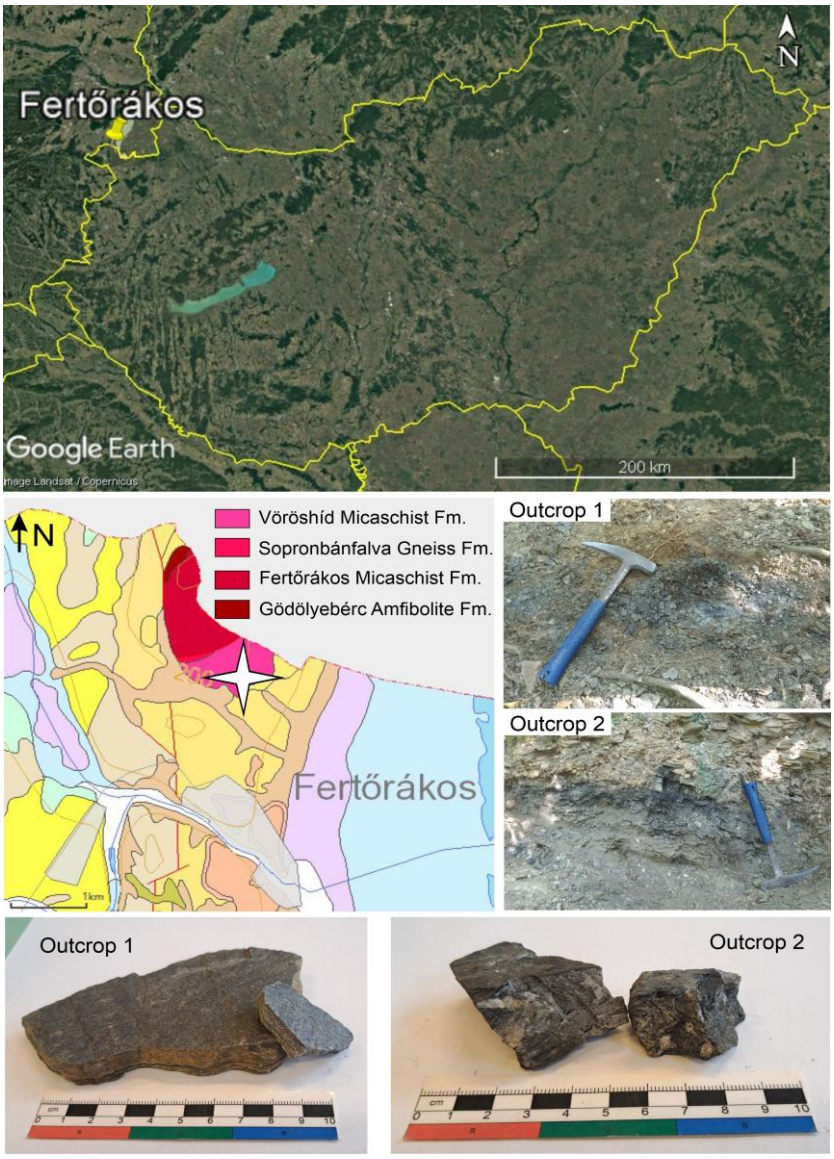

Figure 1

Location map of Fertőrákos village in the Sopron Mts. (top panel). Schematic geological map of the investigated area (online geological map of the Supervisory Authority for Regulatory Affairs, Gyalog and Síkhegyi 2005) (middle left panel). The location of the sample is marked with a white star on the geological map (middle right panel). The surface outcrops and the collected rock samples (bottom panels)

3. RESULTS

3.1. OM and SEM-EDX

Based on OM and SEM-EDX observations, the samples have oriented and highly deformed textures with the marks of shearing deformations, alternating black and white bands. The matrix of the samples consists of 100–300 µm sized quartz grains and 50–100 µm sized phyllosilicate plates (chlorite and muscovite). Muscovite is often paragonitized and fengitized, and a low amount of Ti is also associated according to EDX measurements.

Graphite appears as <50 µm sized flakes, and as 50–300 µm sized granular aggregates, forming lenses *(Figure 2)*. These graphitic aggregates are located in the black bands (particularly in the deformed parts), but some larger aggregates also occur in the white bands. EDX measurements show no sulfur content in the graphitic aggregates.

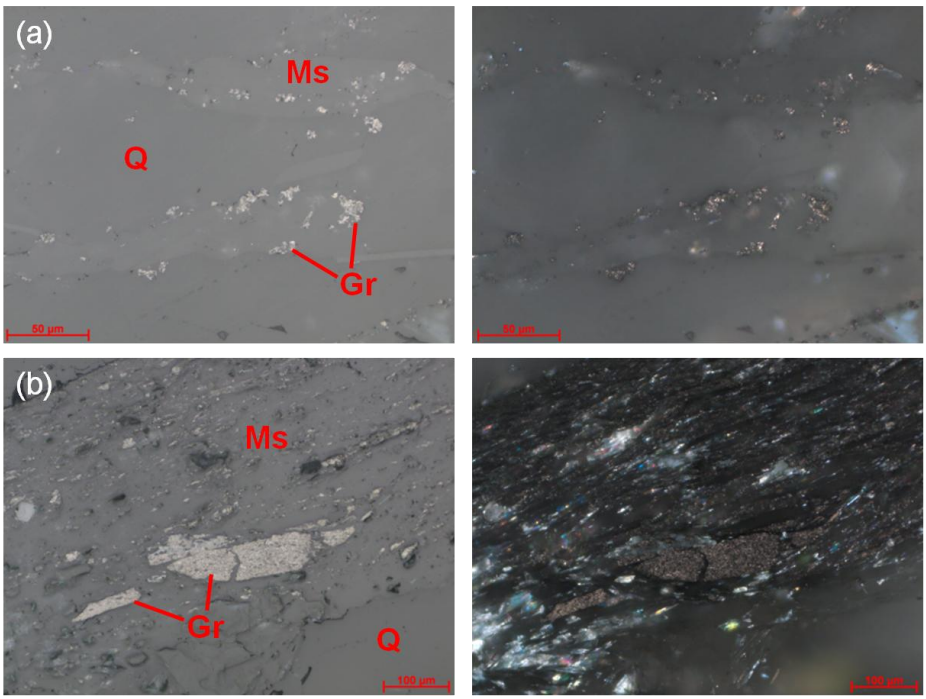

Figure 2

Graphite (Gr) in the quartz (Q) and muscovite (Ms) matrix. Reflected light 1N to the left and XN to the right. (a) Graphite flakes, (b) Graphite flakes and lens-forming graphitic aggregates

The samples contain several accessory minerals. TiO_2 grains with a size of 5–10 µm can be observed scattered in the matrix, and in one place embedded in a fissure-filling smectite. In addition, zircon grains from a few µm to 30 µm in size, monazite-(Ce)

crystals with a size of 10–20 µm, and kaolinite can also be observed in the samples. The monazite-(Ce) grains often have a low Th content based on EDX measurements.

3.2. XRD analysis

The XRD results show quartz rich compositions with trace amounts of muscovite and albite *(Figure 3)*. By XRD, graphite cannot be detected directly on the diffractograms due to its low quantity, nanocrystalline size, preferred orientation and heavy peak overlapping of peak (hkl = 002) between 26°–27°(2θ) with quartz peaks (hkl = 101) and (hkl = 110).

However, by Rietveld refinement, the direct observation and quantification of graphite is possible. *Figure 4* illustrates the calculated quantitative results of the samples.

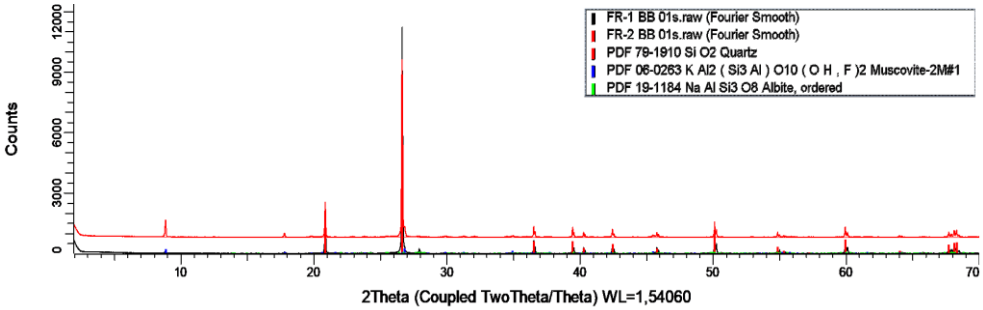

Figure 3
Diffractograms of the Fertőrákos samples

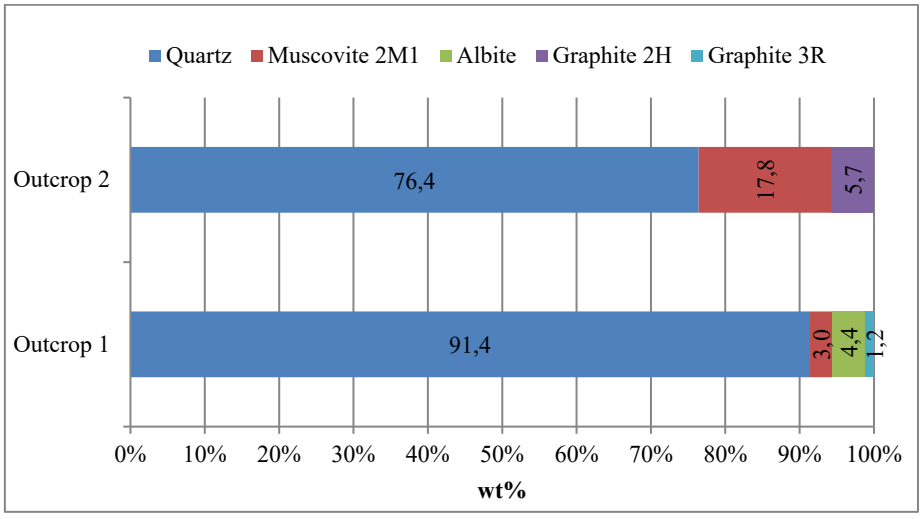

Figure 4
Bar chart of the quantitative results of the Fertőrákos samples by Rietveld refinement (wt%)

3.3. Raman spectroscopy

In the first-order region of the Raman spectrum, two sharp bands can be identified, a higher intensity band at ~1580 cm^{-1} (G band) and a lower intensity band at ~1349 cm^{-1} (D1 band). A low intensity, narrow band at ~1620 cm^{-1} (D2 band) can also be observed as a right shoulder of the G band.

In the second-order region, four bands appear; three bands with low intensity (S1, S3 and S4 bands) and one band with high intensity (S2 band). Furthermore, an initial splitting of the S2 band into two bands (G'_1 and G'_2 bands) can also be observed during the deconvolution. *Figure 5* shows an evaluated Raman spectrum with the first and second-order graphite bands.

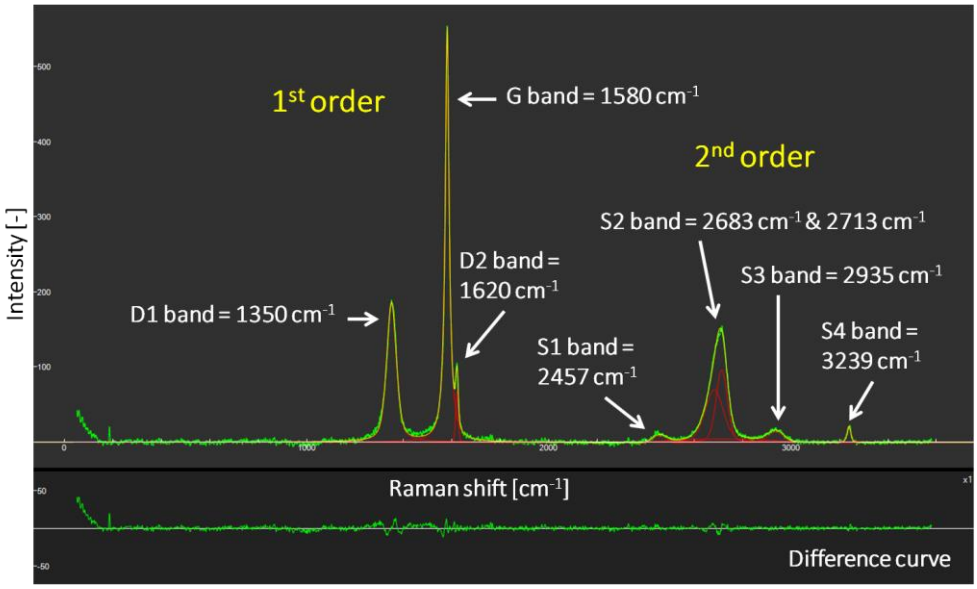

Figure 5

Decomposed Raman spectrum of one measurement point marked with the first and second order bands of graphite

3.4. XRF analysis

By XRF measurements, bulk rock and trace element analysis make it possible to get detailed information about the samples. *Figure 6* shows the major element compositions, while *Figure 7* illustrates the PAAS normalized trace element contents of the samples (PAAS values after Taylor and McLennan 1985). On *Figure 6*, LOI (Loss On Ignition) represents the number of unmeasured elements.

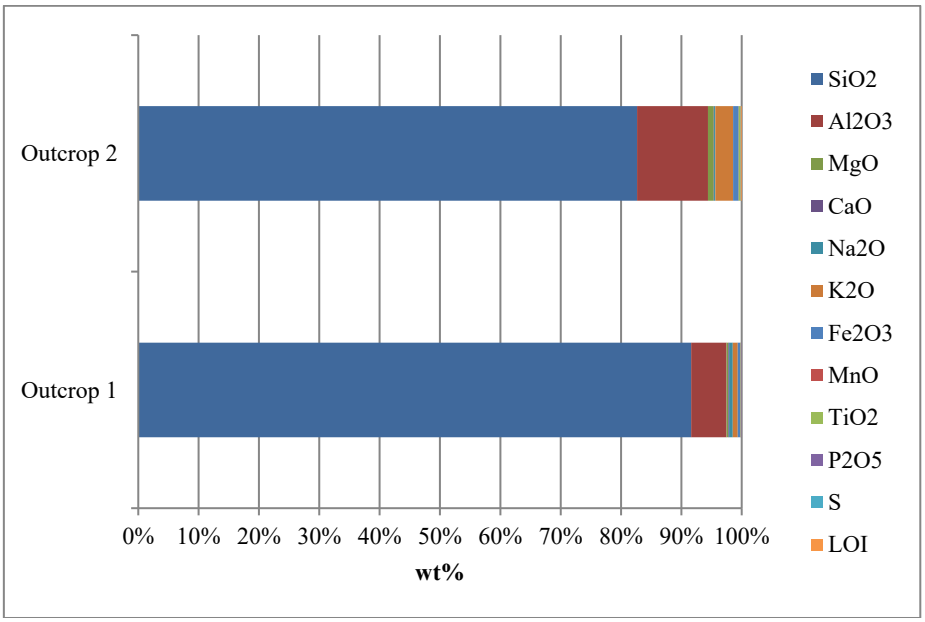

Figure 6
Bar chart of the results of bulk rock analysis by XRF

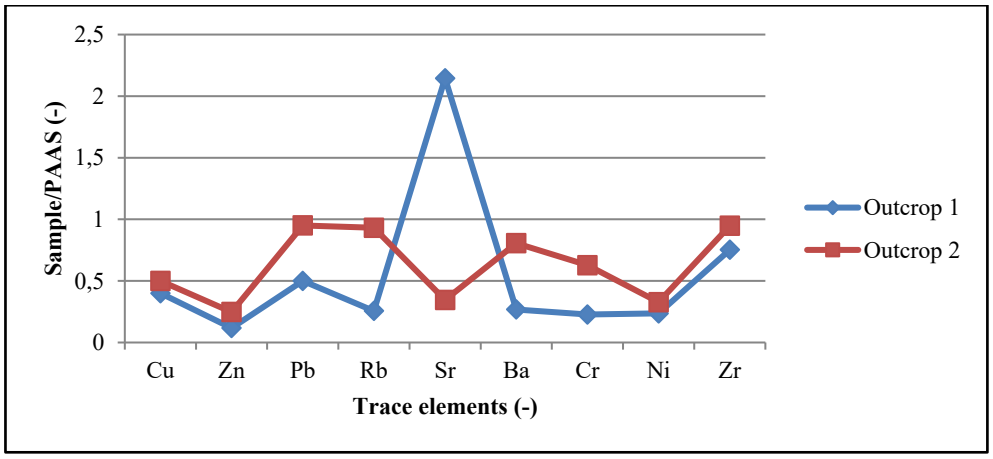

Figure 7
PAAS normalized spider diagram of the results of trace element analysis by XRF
(PAAS values after Taylor and McLennan 1985)

The result of bulk rock analysis by XRF is in accordance with the observations of OM, SEM-EDX and XRD, as it shows quartz rich compositions, the Al, K, Mg, Na and Fe content is related to phyllosilicates (muscovite and chlorite). Ti content is related to TiO_2 and Ti-bearing muscovite, while P content is related to monazite-(Ce). The PAAS normalized trace element analysis by XRF shows a strong positive

Sr anomaly in the sample of outcrop 1, and moderate enrichment of Pb, Rb and Ba in the sample of outcrop 2, and Zr in the samples of both outcrops.

4. DISCUSSION AND CONCLUSIONS

According to our results, graphite cannot be detected directly on diffractograms mainly due to its low quantity and overlapping peaks with quartz peaks. However, its direct quantification is possible by Rietveld refinement; the Fertőrákos samples have 1–5 wt% graphite content. By ore microscopy, graphite flakes and granular aggregates are evidenced in the samples. EDX measurements show no sulfur content in the graphite.

Using Raman spectroscopy, the degree of graphitization of carbonaceous material and the crystallinity of graphite can be identified (Beny-Bassez and Rouzaud, 1985). As both G and D bands appear on the 1st order Raman spectra, and a higher I_G/I_D intensity ratio was detected, the samples contain disordered graphite.

Moreover, Raman spectroscopy is also suitable for determining the peak formation temperature (Henry et al., 2019). One of the parameters required for this is the R2 area ratio value, which can be calculated based on the following equation

$$R2 = D1/(G + D1 + D2), \tag{1}$$

where G is G band area, D1 is D1 band area, D2 is D2 band area.

At first, we used the formula of Beyssac et al. (2002) to calculate the peak formation temperature

$$T(°C) = -445 * R2 + 641\ (\pm 50\ °C) \tag{2}$$

which gives the maximum temperature between 330 and 650 °C. Although *Equation (2)* is developed for graphite formed during regional metamorphism, it uses 514.5 nm laser. However, our measurements were made with 532 nm laser, so we also looked for another equation that also uses 532 nm laser. Thus, we used the formula of Aoya et al. (2010)

$$T(°C) = 221 * (R2)^2 - 637.1 * R2 + 672.3\ (\pm 50\ °C) \tag{3}$$

which is valid between 340 and 655 °C and was developed for contact metamorphic rocks. According to the findings of Aoya et al. (2010), the main effect of using lasers with different wavelengths (514.5 nm and 532 nm) is the systematically greater R2 area ratios obtained with a 532-nm laser. The degree of this effect corresponds to a temperature difference of less than 10 °C. This is in accordance with the findings of Lünsdorf et al. (2014), who investigate all biasing factors to obtain more comparable geothermometric data. Based on their study, three main sources can modify the formation temperature values: spectral curve-fitting procedure, the sample characteristics itself and the Raman system configuration. Taking every biasing factor into account, Lünsdorf et al. (2014) demonstrated that the total difference of all errors is

~10–30 °C, which is below the given error of ±50 °C of Beyssac et al. (2002) and Aoya et al. (2010). Aoya et al. (2010) also concluded that any equation can be used for peak formation temperature calculations (*Equation 2* or *3*) as the error range is ±50 °C. *Table 1* contains the average value of R2 and the formation temperature results calculated using the two formulas.

Table 1

The calculated average R2 area ratio value, the average peak formation temperatures (±50 °C) using the two formulas, and the difference between the calculated temperature values

R2 value [–]	Temperature calculated by the formula of Beyssac et al. (2002) [°C]	Temperature calculated by the formula of Aoya et al. (2010) [°C]	Difference [°C]
0.44	443	434	9

By graphite geothermometry, the average formation temperature of the Fertőrákos samples is ~440 °C (±50 °C), which fits the known geological background of the area, as the Fertőrákos Metamorphic Complex underwent greenschist facies metamorphism (Babinszki et al., 2024).

Due to the metamorphic texture of the samples and the appearance of graphite in the highly deformed zones detected by OM and SEM-EDX, the formation of graphite is connected to shear zones and regional metamorphism.

The high Sr and Ba anomalies, detected by XRF, may indicate fluid-rock interaction. Their enrichment may suggest metasomatic alteration or involvement of a fluid phase during metamorphism (Casillas et al., 2011). The elevated Zr content might suggest the preservation of inherited zircon crystals from the protoliths.

As a conclusion, the joint usage of the applied analytical techniques (ore microscopy, scanning electron microscopy, Raman spectroscopy, X-ray powder diffraction and X-ray fluorescence spectrometry), is a good tool to investigate graphite-bearing samples: texture, mineral paragenesis, crystalline phases, chemical composition, degree of graphitization and peak formation temperature.

REFERENCES

Aoya, M., Kouketsu, Y., Endo, S., Shimizu, H., Mizukami, T., Nakamura, D., Wallis, S. (2010). Extending the applicability of the Raman carbonaceous material geothermometer using data from contact metamorphic rocks. *Journal of Metamorphic Geology*, 28, pp. 895–914. https://doi.org/10.1111/j.1525-1314.2010.00896.x

Babinszki, E., Piros, O., Budai, T., Gyalog, L., Halász, A., Király, E., Koroknai, B., Lukács, R., M. Tóth, T. (eds.) (2024). *Lithostratigraphic units of Hungary I. Pre-Cenozoic formations.* Budapest, Supervisory Authority for Regulatory Affairs.

Beny-Bassez, C., Rouzaud, J. N. (1985). Characterization of carbonaceous materials by correlated electron and optical microscopy and Raman microspectroscopy. *Scanning Electron Microscopy*, 1, pp. 119–132.

Beyssac, O., Goffé, B., Chopin, C., Rouzaud, J. N. (2002). Raman spectra of carbonaceous material in metasediments: a new geothermometer. *Journal of Metamorphic Geology*, 20, pp. 859–871. https://doi.org/10.1046/j.1525-1314.2002.00408.x

Casillas, R., Demény, A., Nagy, G., Ahijado, A., Fernández, C. (2011). Metacarbonatites in the Basal Complex of Fuerteventura (Canary Islands). The role of fluid/rock interactions during contact metamorphism and anatexis. *Lithos*, 125 (1–2), pp. 503–520. https://doi.org/10.1016/j.lithos.2011.03.007

Downs, R. T., Hall-Wallace, M. (2003). The American Mineralogist Crystal Structure Database. *American Mineralogist*, 88, pp. 247–250.

Gyalog, L., Síkhegyi, F. (series editor) (2005). *Geological Map of Hungary, 1:100 000.* Published by the Hungarian National Geological Institute, Budapest. Available online: https://map.hugeo.hu/fdt100/, (accessed on 04 May 2025).

Henry, D. G., Jarvis, I., Gillmore, G., Stephenson, M. (2019). Raman spectroscopy as a tool to determine the thermal maturity of organic matter: Application to sedimentary, metamorphic and structural geology. *Earth-Science Reviews*, 198, 102936, 19 p. https://doi.org/10.1016/j.earscirev.2019.102936

Kósa, L., Fazekas, V. (1981). Geological and petrological structure of the Fertőrákos crystalline schist complex (in Hungarian). *Földtani Közlöny*, 111, pp. 424–452.

Leskóné Majoros, L., Leskó, M. Zs., Szakáll, S., Kristály, F. (2021). Critical minerals and elements in the Szendrő Phyllite Formation (Szendrő Mts., NE-Hungary) (in Hungarian). *Multidisciplinary Sciences*, 11 (1), pp. 90–97. https://doi.org/10.35925/j.multi.2021.1.9

Leskóné Majoros, L., Leskó, M. Zs., Fintor, K., Szakáll, S., Kristály, F. (2022). Graphite occurrences in NE-Hungary. In: Szabó N. P., Virág Z. (eds.). *Új eredmények a műszaki föld- és környezettudományban 2022.* Miskolc-Egyetemváros, Miskolci Egyetem, Műszaki Földtudományi Kar, pp. 49–56.

Lünsdorf, N. K., Dunkl, I., Schmidt, B. C., Rantitsch, G., von Eynatten, H. (2014). Towards a Higher Comparability of Geothermometric Data obtained by Raman Spectroscopy of Carbonaceous Material. Part I: Evaluation of Biasing Factors. *Geostandards and Geoanalytical Research*, 38 (1), pp. 73–94. https://doi.org/10.1111/j.1751-908X.2013.12011.x.

Majoros, L. (2019). *Mineralogical and petrographical examinations of graphitic materials in black schists from Uppony Mts and Szendrő Mts and their Carpathian connections* (in Hungarian). University of Miskolc, Institute of Mineralogy and Geology, MSc diploma thesis, 102 p.

Majoros, L., Fintor, K., Koós, T., Szakáll, S., Kristály, F. (2022). Metamorphic graphite from Szendrőlád (Szendrő Mts., NE-Hungary) detected by simultaneous DTA-TG. *Journal of Thermal Analysis and Calorimetry*, 147, 3417–3425. https://doi.org/10.1007/s10973-021-10713-6

Study on the Critical Raw Materials for the EU 2023. Final Report. European Commission. https://doi.org/10.2873/725585

Taylor, S. R., McLennan, S. M. (1985). *The Continental Crust: Its Composition and Evolution.* Oxford, UK, Blackwell.